Pergamon

J. Quant. Spectrosc. Radiat. Transfer Vol. 55, No. 5, pp. 683–694, 1996

S0022-4073(96)00011-8
0022-4073/96 $15.00 + 0.00

ELECTROMAGNETIC SCATTERING BY RANDOMLY ORIENTED BISPHERES: COMPARISON OF THEORY AND EXPERIMENT AND BENCHMARK CALCULATIONS

MICHAEL I. MISHCHENKO†[a] and DANIEL W. MACKOWSKI[b]

[a]NASA Goddard Institute for Space Studies, 2880 Broadway, New York, NY 10025 and
[b]Department of Mechanical Engineering, Auburn University, Auburn, AL 36849-5341, U.S.A.

Abstract—A good quantitative agreement is found between laboratory measurements of the scattering matrix for a randomly oriented latex bisphere with touching, nearly identical micron-sized components and theoretical computations using the T-matrix method. Our comparison of theory and experiment provides an additional validation of the computational method and also demonstrates that polarization measurements of light scattering can be employed as an accurate particle sizing technique. The T-matrix method is used to tabulate light scattering properties of two different kinds of randomly oriented bispheres with touching and separated components. Because of high accuracy, our computations can serve as benchmarks.

1. INTRODUCTION

Controlled laboratory measurements‡ of the scattering matrix are often considered an important test in validating theoretical techniques for computing light scattering by small nonspherical particles. For example, Kattawar and Dean[1] and Fuller et al[2] compared laboratory measurements of light scattering by bispheres (two-sphere aggregates) in a fixed orientation with theoretical computations using the superposition approach. Kattawar et al[3] used laboratory scattering data for cubical particles to validate their resolvent kernel technique. Hage et al[4] compared numerical computations using the so-called volume integral equation formulation with laboratory scattering measurements for an irregular porous cube.

In 1980, Bottiger et al[5] published the results of a unique laboratory study of the scattering matrix for randomly oriented aggregates composed of nearly identical micron-sized latex spheres. The number of component spheres in a cluster varied from 1 to 4. To the best of our knowledge, those measurements have never been analysed theoretically because of substantial difficulties in computing the scattering of light by randomly oriented multiple-sphere aggregates. Recently, however, Mishchenko and Mackowski[6] have developed an efficient T-matrix method for rigorously calculating the scattering matrix for randomly oriented bispheres with sizes comparable to the wavelength of light.§ Therefore, it is the primary purpose of this paper to compare, for the first time, the laboratory measurements of Bottiger et al[5] for randomly oriented bispheres (i.e., two-sphere clusters with touching components) with theoretical computations.

Our second purpose is to tabulate results of accurate T-matrix computations of light scattering by randomly oriented bispheres. Most theoretical methods for calculating nonspherical particle scattering, especially for particles in random orientation, are complicated and result in large, sophisticated, and time-consuming computer codes. Testing such codes requires accurate numerical data in the form of reproducible benchmark results. Some benchmark computations of this type have been reported recently for randomly oriented spheroids and Chebyshev particles by Mishchenko[7,8] and Kuik et al.[9] In this paper we extend the existing set of benchmark nonspherical

†To whom all correspondence should be addressed.

‡The term 'controlled laboratory measurements' means that accurate measurements of light scattering are accompanied by a precise specification of the particle size, shape, refractive index, and orientation.

§Note that Ref. 6 contains a typographical error. Specifically, the second sentence of the last paragraph on page 1605 should read as follows: The index of refraction of the spheres is $1.5 + 0.02i$ and the size parameter of each sphere is 15.874.

calculations by accurately computing the optical efficiency factors and the elements of the scattering matrix for monodisperse, randomly oriented bispheres with touching and separated components.

2. COMPARISON OF THEORETICAL COMPUTATIONS WITH LABORATORY DATA

Bottiger et al[5] used an electrostatic levitation technique to suspend a particle in air and measured ratios of the elements of the Mueller scattering matrix relative to its (1,1)-element as functions of the scattering angle Θ in the range $12° \leqslant \Theta \leqslant 165°$. The Mueller scattering matrix $\mathbf{Z}$ transforms the Stokes vector of the incident light $\mathbf{I}^{\text{inc}} = \{I^{\text{inc}}, Q^{\text{inc}}, U^{\text{inc}}, V^{\text{inc}}\}$ into the Stokes vector of the scattered light $\mathbf{I}^{\text{sca}} = \{I^{\text{sca}}, Q^{\text{sca}}, U^{\text{sca}}, V^{\text{sca}}\}$ according to the relationship

$$\mathbf{I}^{\text{sca}} = \frac{1}{R^2}\mathbf{Z}(\Theta)\mathbf{I}^{\text{inc}}, \tag{1}$$

where the Stokes parameters I, Q, U, and V have the dimension of the monochromatic energy flux, Θ is the scattering angle (i.e., the angle between the incident and scattered beams), R is the distance between the scattering particle and observation point, and the Stokes vectors $\mathbf{I}^{\text{inc}}$ and $\mathbf{I}^{\text{sca}}$ are assumed to be specified with respect to the scattering plane (i.e., the plane through the incident and the scattered beams). As the source of light, Bottiger et al used a He–Cd laser operating at a wavelength of 441.6 nm. The electrostatic levitation technique enabled Bottiger et al to select a single scattering particle (a latex sphere or a cluster of spheres) and trap it in a very small volume. The particle was subject to Brownian motion and rapidly changed its orientation. Therefore, although the sample was a single particle, the measurements of the scattering matrix elements were equivalent to those for randomly oriented monodisperse particles. According to Bottiger et al this was indeed the case corroborated by simultaneous measurements of the ratios Z_{13}/Z_{11}, Z_{14}/Z_{11}, Z_{23}/Z_{11}, Z_{24}/Z_{11}, Z_{31}/Z_{11}, Z_{32}/Z_{11}, Z_{41}/Z_{11}, and Z_{42}/Z_{11} which were found to be zero within the (unspecified) experimental accuracy, as it would be for randomly oriented particles having a plane of symmetry.[10]

Note that for randomly oriented particles with a plane of symmetry, the Mueller scattering matrix in the transformation law of Eq. (1) is traditionally replaced by the normalized scattering matrix $\mathbf{F}$ given by

$$\mathbf{F}(\Theta) = \begin{bmatrix} F_{11}(\Theta) & F_{12}(\Theta) & 0 & 0 \\ F_{12}(\Theta) & F_{22}(\Theta) & 0 & 0 \\ 0 & 0 & F_{33}(\Theta) & F_{34}(\Theta) \\ 0 & 0 & -F_{34}(\Theta) & F_{44}(\Theta) \end{bmatrix} = \frac{4\pi}{C_{\text{sca}}}\mathbf{Z}(\Theta), \tag{2}$$

where C_{sca} is the scattering cross section and the (1,1) element satisfies the normalization condition

$$\frac{1}{4\pi}\int_{4\pi} \mathrm{d}\Omega F_{11}(\Theta) = 1. \tag{3}$$

Since the measurements of Bottiger et al[5] pertain to a randomly oriented bisphere, in what follows we will adopt this tradition and use $\mathbf{F}$ instead of $\mathbf{Z}$.

Unfortunately, Bottiger et al[5] did not measure the size of the particles for which they obtained their scattering data and only indicate that the average diameter of latex microspheres used in their experiments was 1091 nm with standard deviation 8 nm. Our T-matrix computations for a randomly oriented bisphere with the monomer sphere diameter of 1091 nm and refractive index of 1.588[11] showed no resemblance to the Bottiger et al data. However, we have found that the theoretical scattering pattern is strongly dependent on the particle size, and that a good agreement can be obtained for monomer sphere diameters slightly different from 1091 nm. Therefore, we decided to consider the monomer diameter a free parameter and determined this parameter by repeating computations with a small diameter step size and looking for the best fit to the laboratory data. An excellent fit was obtained for the monomer dia 1129 nm, as demonstrated in Fig. 1. The overall agreement is very good, especially for the ratios F_{33}/F_{11}, F_{44}/F_{11}, F_{12}/F_{11}, and F_{34}/F_{11}. The

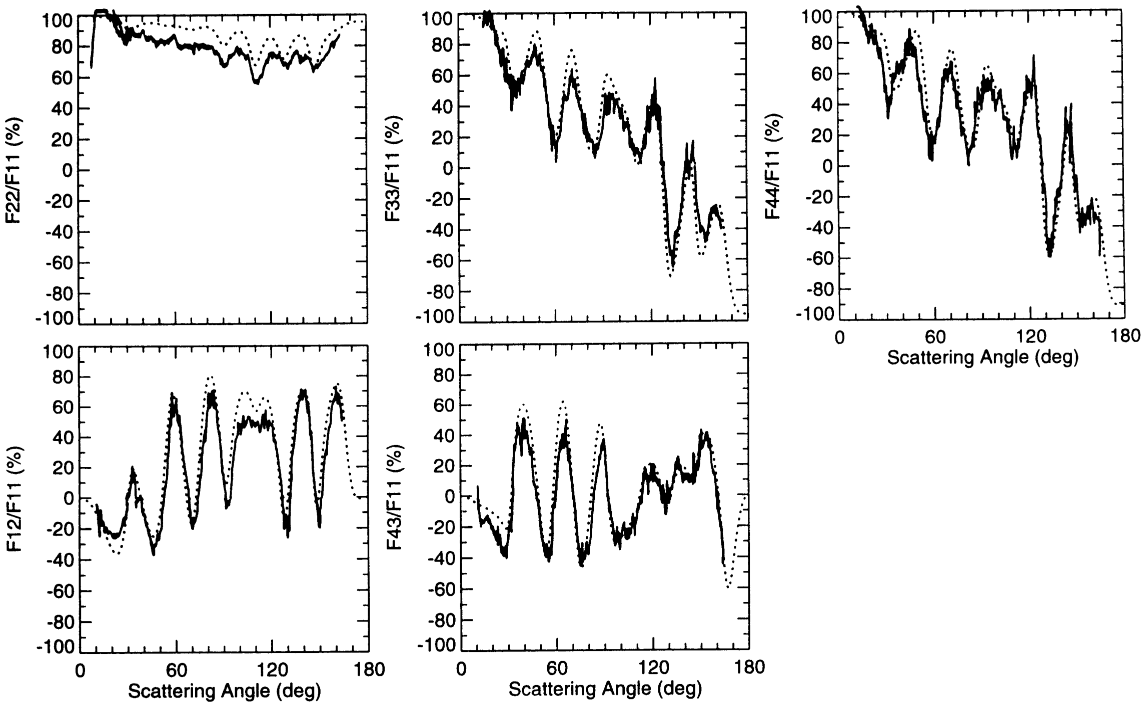

Fig. 1. Ratios of the elements of the scattering matrix for a latex bisphere in random orientation. (——) Measurements of Bottiger et al.[5] (· · · · · ·) T-matrix computations for the monomer sphere dia 1129 nm.

residual differences between measurements and computations are somewhat larger for the ratio F_{22}/F_{11} than for other ratios, and it is not clear at this point whether or not all of those differences can be attributed to experimental errors. The absolute accuracy of computing the ratios of the scattering matrix elements theoretically was better than 10^{-3}. On the other hand, Bottiger et al do not indicate the measurement accuracy of their data. It is obvious, however, that the measurements at small scattering angles violate the general inequality[12] $|F_{ij}|/F_{11} \leqslant 1$ and that this violation must

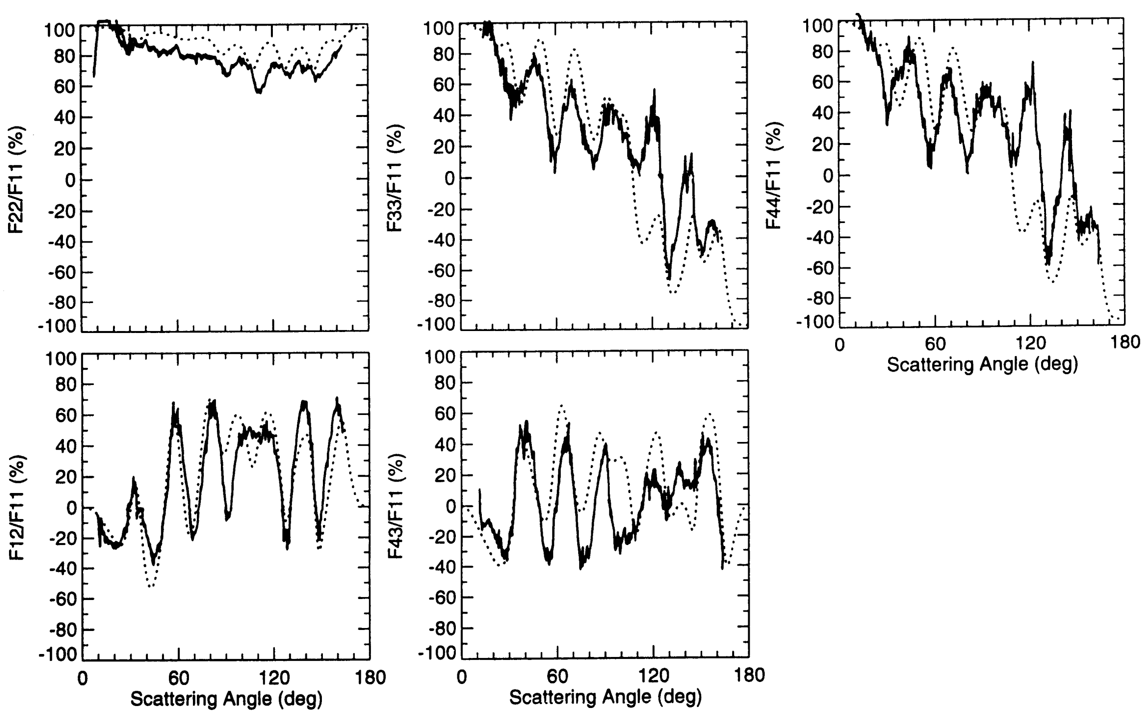

Fig. 2. As in Fig. 1, but (· · · · · ·) show theoretical computations for the monomer sphere dia 1108 nm.

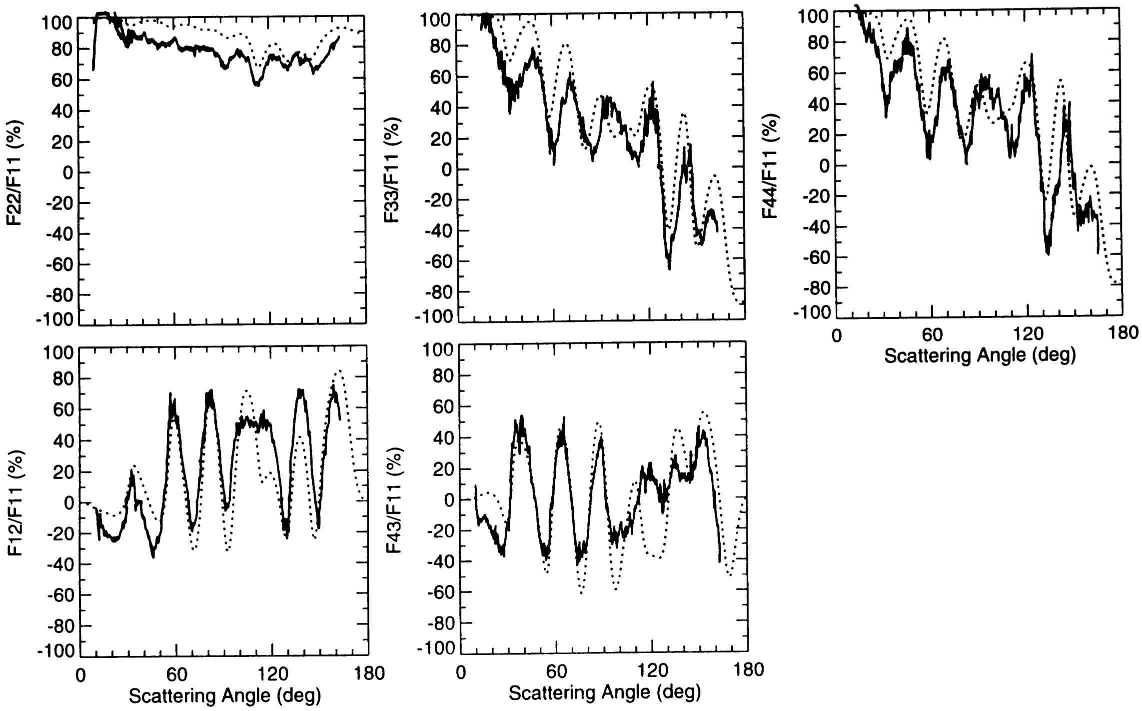

Fig. 3. As in Fig. 1, but (······) show theoretical computations for the monomer sphere dia 1150 nm.

be fully attributed to experimental errors. It should also be noted that we could not obtain a better agreement between theoretical computations and measurements by using a bisphere with a slightly different refractive index or with slightly unequal components. Importantly, as Figs. 2 and 3 demonstrate, no acceptable solution can be found for monomer diameters smaller than 1108 nm and larger than 1150 nm. For comparison, Fig. 4 shows the best fit of Mie computations to

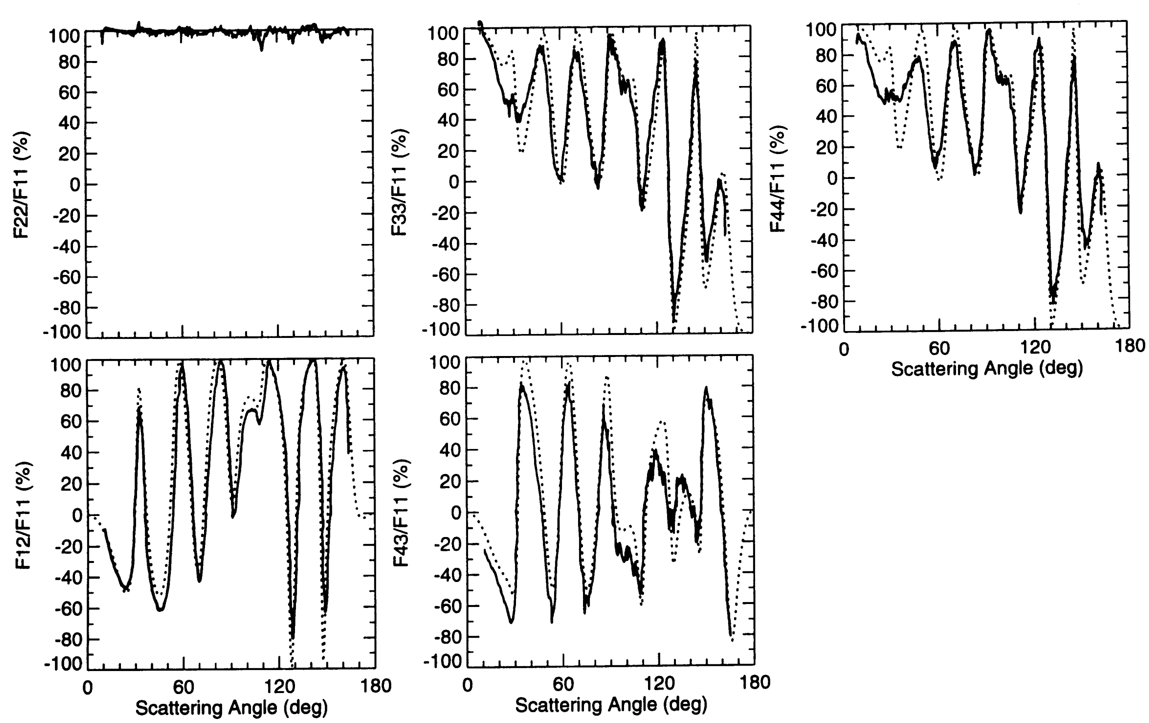

Fig. 4. Ratios of the elements of the scattering matrix for a single latex sphere. (——) Measurements of Bottiger et al.[5] (······) Computed using Mie theory for the sphere dia 1122 nm.

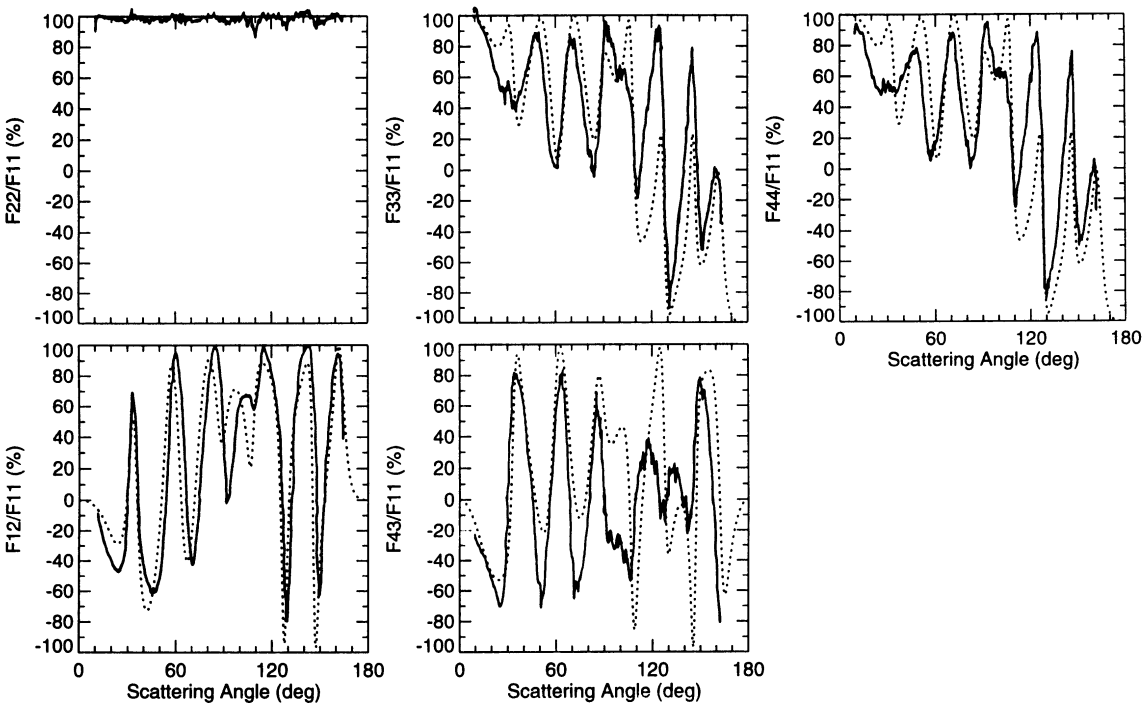

Fig. 5. As in Fig. 4, but (· · · · · ·) show theoretical computations for the sphere dia 1108 nm.

measurements of Bottiger et al for a single latex sphere (note that for spherical particles the ratio F_{22}/F_{11} must be identically equal to 1). This fit was obtained for the sphere dia 1122 nm, which is again somewhat different from the average diameter of the latex microspheres as reported by Bottiger et al.[5] As Figs. 5 and 6 demonstrate, the uncertainty in the sphere diameter determined by comparing theoretical computations with laboratory measurements is very small. Thus, our

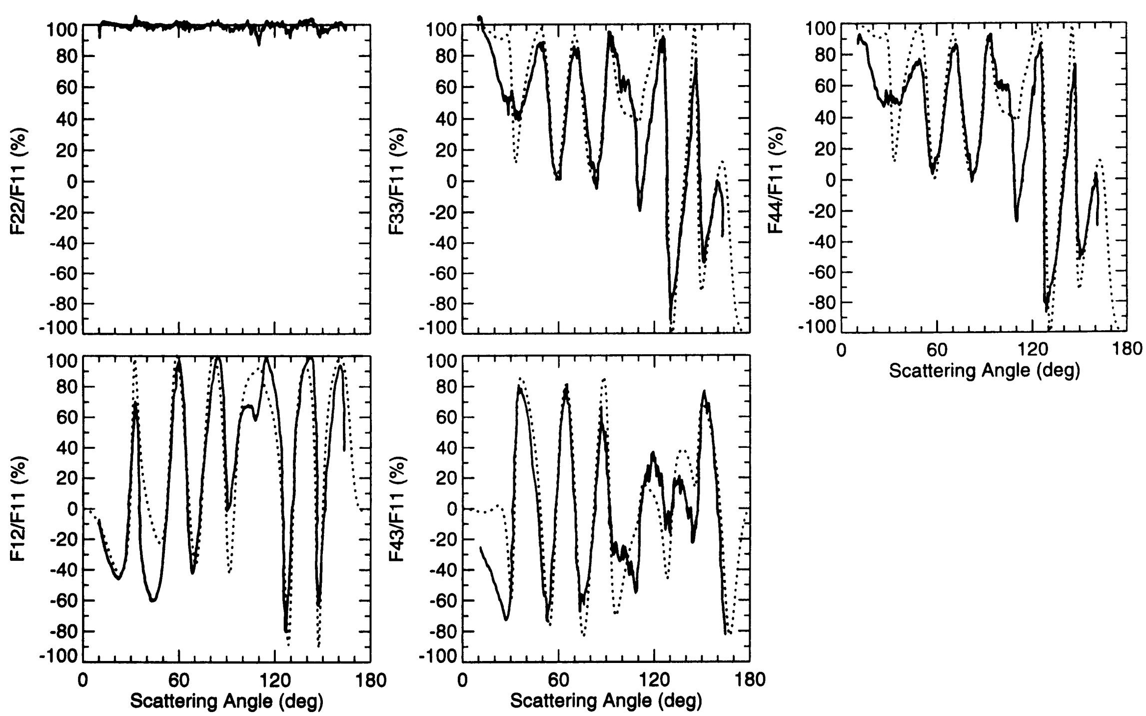

Fig. 6. As in Fig. 4, but (· · · · · ·) show theoretical computations for the sphere dia 1136 nm.

comparisons not only demonstrate a good agreement between theory and experiment and thus further validate the T-matrix method for randomly oriented bispheres, but also suggest that experimental measurements of the scattering matrix can be used as an accurate particle sizing technique.

3. BENCHMARK RESULTS

Besides the above experimental validation and the easily controllable internal convergence of the T-matrix method, the accuracy of our T-matrix code[6] is demonstrated by the following additional tests.

(1) Our computations of the normalized scattering matrix elements for randomly oriented bispheres are in full agreement with general equalities[10,13,14] $F_{12}(0) = F_{12}(\pi) = F_{34}(0) = F_{34}(\pi) = 0$, $F_{22}(0) = F_{33}(0)$, $F_{22}(\pi) = -F_{33}(\pi)$, $F_{11}(\pi) - F_{22}(\pi) = F_{44}(\pi) - F_{33}(\pi)$, and $F_{11}(0) - F_{22}(0) = F_{33}(0) - F_{44}(0)$, as well as with general inequalities for the elements of the scattering matrix[12,15] and for the expansion coefficients appearing in expansions of these elements in generalized spherical functions [see Eqs. (4)–(6) below].[16]

(2) T-matrix computations for a bisphere with components of different size converge to the regular Mie solution for the bigger component as the size of the smaller component approaches zero.

(3) T-matrix computations for a bisphere with increasing distance between identical components converges to the Mie solution for independent spheres.[17] The only exception is the direction of exact forward scattering where the interference of light singly scattered by the bisphere components is constructive for any bisphere orientation and nearly doubles the height of the forward-scattering phase function peak as compared to that of a single sphere.

(4) The computation of the T-matrix for a bisphere in the particle coordinate system with the z-axis connecting the component sphere centers requires the specification of the size parameters of the upper and lower components. If the size parameters are different, one has a choice of assigning the larger size parameter to the upper or to the lower sphere. However, the scattering results for randomly oriented bispheres must be independent of the choice, and, indeed, our code produces the same results whatever the choice is. Similarly, bisphere components can have different refractive indices, and our code produces results which do not depend on assigning a particular refractive index to the upper or to the lower component.

(5) For nonabsorbing particles (imaginary part of the refractive index equals zero) the scattering and extinction cross sections must be equal. Our T-matrix code reproduces this equality with very high accuracy.

(6) The T-matrix method, as described by Mishchenko and Mackowski,[6] includes the computation of the bisphere T-matrix as a first step and then the use of this T-matrix in an analytical procedure to compute the orientationally averaged light scattering characteristics for randomly oriented bispheres. Alternatively, the T-matrix can also be used to compute light scattering by the bisphere in a fixed orientation. We have tested the accuracy of computing the bisphere T-matrix by using numerical data for a fixed bisphere orientation by Flatau et al,[18,19] who employed a different computational technique,[20] and found agreement of up to 4 significant digits. The analytical averaging procedure has been extensively tested before in computations for randomly oriented spheroids and Chebyshev particles.[7–9]

(7) Our T-matrix computations of the phase function and the degree of linear polarization for randomly oriented bispheres with touching and separated components show agreement of up to three significant digits with calculations of Tishkovets[21] who employed the standard orientation averaging method based on numerical angle integrations.

Our tests show that the internal accuracy of the T-matrix method (i.e., convergence of computations to the same result with increasing length of field expansions in vector spherical functions) is a good measure of its absolute accuracy. This allows us to believe that our T-matrix code is capable of producing very accurate numerical results for randomly oriented bispheres. Below we use our code to tabulate results of computations for the following two models.

(i) Model 1—monodisperse, randomly oriented bispheres with touching identical components having the size parameter 10.

Table 1. Efficiency factors for extinction Q_{ext} and scattering Q_{sca} and asymmetry parameters of the phase function $\langle \cos \Theta \rangle$ for Models 1 and 2.

	Q_{ext}	Q_{sca}	$\langle \cos\Theta \rangle$
Model 1	5.00867	4.54044	0.773159
Model 2	7.49960	7.22024	0.717082

Table 2. Expansion coefficients for Model 1.

s	a_1^s	a_2^s	a_3^s	a_4^s	b_1^s	b_2^s
0	1.00000	.00000	.00000	.87229	.00000	.00000
1	2.31948	.00000	.00000	2.36907	.00000	.00000
2	3.51529	4.20591	3.94681	3.39903	-.10704	.03722
3	4.12964	4.48530	4.52300	4.26877	.01807	.05421
4	5.13265	5.35018	5.14382	5.08820	.01959	.14724
5	5.73251	5.94005	5.85658	5.70677	.16399	.01082
6	6.38093	6.52847	6.49661	6.37910	.11126	.09008
7	6.76759	6.92868	6.88783	6.75816	.22960	-.07191
8	7.03376	7.23083	7.21766	7.05010	.21180	.05337
9	7.20921	7.31807	7.25545	7.16920	.21680	-.18608
10	7.10937	7.33753	7.35473	7.14526	.22752	-.00121
11	7.06202	7.13119	7.08530	7.04197	.24550	-.24240
12	6.71833	6.96261	6.94211	6.71527	.23003	-.06406
13	6.45893	6.48918	6.49103	6.48071	.33359	-.23288
14	5.96069	6.20824	6.16204	5.93567	.24675	-.08156
15	5.59296	5.58437	5.59052	5.61311	.39411	-.15044
16	5.10813	5.32414	5.29248	5.09937	.34344	-.08839
17	4.96096	4.89087	4.80842	4.87255	.51086	.23109
18	4.82317	4.94825	4.98454	4.84890	.13775	.24034
19	4.68328	4.64281	4.79264	4.85627	-.00036	.21702
20	4.59233	4.74142	4.67444	4.57654	-.04321	-.31954
21	4.16308	4.18599	4.22534	4.25588	.08982	-.21076
22	3.97908	4.09160	3.83552	3.74912	.34001	-.26962
23	3.29696	3.31546	3.35205	3.32126	.08074	.07281
24	3.06576	3.10155	3.10244	3.06039	.07749	-.03904
25	2.73820	2.76744	2.78332	2.74916	.09326	-.04475
26	2.42684	2.45828	2.45964	2.42579	.11769	-.06452
27	2.09463	2.12280	2.13100	2.10168	.12059	-.06366
28	1.78198	1.80877	1.81373	1.78788	.12983	-.07352
29	1.47759	1.50260	1.50454	1.48198	.13625	-.07491
30	1.19423	1.21617	1.21756	1.19901	.13712	-.06903
31	.93817	.95777	.95976	.94466	.13356	-.06507
32	.71207	.72934	.72915	.71746	.12947	-.06251
33	.52269	.53683	.53377	.52559	.12733	-.05294
34	.37714	.38793	.38172	.37661	.12025	-.03299
35	.27098	.27887	.27643	.27398	.09529	-.01406
36	.20142	.20760	.20880	.20858	.06364	-.01364
37	.15459	.16043	.15872	.15947	.04192	-.02816
38	.11533	.12088	.11172	.11237	.03349	-.03746
39	.07520	.07961	.06773	.06802	.02663	-.03315
40	.04419	.04703	.03587	.03591	.02097	-.02134
41	.02066	.02213	.01571	.01567	.01194	-.01007
42	.00918	.00982	.00635	.00631	.00647	-.00388
43	.00320	.00344	.00216	.00214	.00255	-.00104
44	.00114	.00122	.00074	.00073	.00099	-.00023
45	.00033	.00035	.00022	.00022	.00029	-.00001
46	.00010	.00011	.00007	.00007	.00009	.00001
47	.00003	.00003	.00002	.00002	.00002	.00001
48	.00001	.00001	.00001	.00001	.00000	.00000

(ii) Model 2—monodisperse, randomly oriented bispheres with identical separated components having the size parameter 5. The distance between the sphere centers is 2 times their diameter.

For both models, the index of refraction is $1.5+0.005i$. Table 1 shows the efficiency factors for extinction Q_{ext} and scattering Q_{sca} and the asymmetry parameter of the phase function $\langle \cos\Theta \rangle$. The efficiency factors are defined as the corresponding cross sections divided by the geometrical cross section of the monomer sphere. Tables 2 and 3 show the expansion coefficients that appear in the following expansions of the elements of the normalized scattering matrix in generalized spherical functions[7,22]

$$F_{11}(\Theta)=\sum_{s=0}^{s_{max}} a_1^s P_{00}^s(\cos\Theta), \tag{4}$$

$$F_{22}(\Theta)+F_{33}(\Theta)=\sum_{s=2}^{s_{max}} (a_2^s+a_3^s)P_{22}^s(\cos\Theta), \tag{5}$$

$$F_{22}(\Theta)-F_{33}(\Theta)=\sum_{s=2}^{s_{max}} (a_2^s-a_3^s)P_{2,-2}^s(\cos\Theta), \tag{6}$$

Table 3. Expansion coefficients for Model 2.

s	a_1^s	a_2^s	a_3^s	a_4^s	b_1^s	b_2^s
0	1.00000	.00000	.00000	.94160	.00000	.00000
1	2.15125	.00000	.00000	2.21375	.00000	.00000
2	2.99437	4.00361	3.83857	2.89376	-.13647	.11745
3	3.13877	3.55605	3.63214	3.20301	-.11917	.00216
4	3.32190	3.77498	3.68288	3.26877	-.15255	.10368
5	3.32936	3.46499	3.50235	3.40753	-.19897	-.04975
6	3.18348	3.58119	3.45692	3.09234	-.23832	.00832
7	2.95333	2.98997	3.11209	3.13450	-.27378	-.06001
8	2.47715	2.91924	2.73441	2.37083	-.43506	-.33890
9	1.94766	1.95517	1.99875	2.03174	-.08178	-.21840
10	1.62692	1.85138	1.74819	1.56046	-.15704	-.30807
11	1.20454	1.22355	1.22116	1.20713	.04472	-.06978
12	1.27983	1.27994	1.27321	1.27673	.01441	-.00550
13	1.39985	1.39649	1.39540	1.40073	.01718	.01608
14	1.52960	1.52807	1.52819	1.53191	.01704	.02120
15	1.66183	1.65843	1.65642	1.66209	.02479	.02294
16	1.79873	1.79692	1.79303	1.79602	.03754	.01614
17	1.88397	1.89037	1.88688	1.87990	.04223	.01045
18	1.87931	1.89487	1.89122	1.87306	.04009	.00650
19	1.77319	1.79585	1.79750	1.77103	.02763	.00827
20	1.59409	1.62019	1.62268	1.59283	.00972	.00493
21	1.37720	1.40242	1.40635	1.37793	-.00433	.00240
22	1.15582	1.17893	1.18291	1.15756	-.01639	-.00189
23	.93894	.95986	.96444	.94251	-.02933	-.00688
24	.73777	.75635	.75982	.74154	-.03810	-.01711
25	.55240	.56872	.57051	.55550	-.03998	-.02786
26	.38710	.40096	.40023	.38810	-.03397	-.03530
27	.24605	.25677	.25475	.24563	-.02365	-.03396
28	.14064	.14780	.14516	.13914	-.01241	-.02673
29	.06992	.07398	.07220	.06878	-.00530	-.01628
30	.03132	.03330	.03213	.03048	-.00145	-.00876
31	.01211	.01294	.01241	.01172	-.00016	-.00377
32	.00430	.00460	.00437	.00411	.00013	-.00148
33	.00133	.00143	.00135	.00127	.00011	-.00049
34	.00038	.00041	.00039	.00036	.00005	-.00015
35	.00010	.00011	.00010	.00009	.00002	-.00004
36	.00002	.00003	.00002	.00002	.00001	-.00001
37	.00001	.00001	.00001	.00000	.00000	.00000

Table 4. Elements of the normalized scattering matrix vs scattering angle (in degrees) for Model 1.

Θ	F_{11}	F_{22}	F_{33}	F_{44}	F_{12}	F_{34}
0	141.95599	141.89114	141.89114	141.82628	.00000	.00000
5	86.10333	86.04588	86.03168	85.97577	-1.43941	.56077
10	22.65641	22.61184	22.56340	22.52308	-1.41976	.31853
15	8.22474	8.19201	8.11851	8.09346	-1.05936	.17276
20	2.91107	2.88527	2.82383	2.80970	-.50705	.21758
25	.71746	.69480	.64952	.64016	-.00656	-.00965
30	.96433	.94244	.82932	.81965	-.06293	-.35538
35	1.37174	1.35106	1.26601	1.25723	-.16996	-.38835
40	1.07417	1.05524	1.02919	1.02433	-.09034	.02292
45	.50852	.49031	.36000	.35740	.18777	.06693
50	.58944	.57104	.40922	.40539	.17576	-.26147
55	.69690	.67886	.61954	.61637	-.04314	-.18515
60	.48878	.47107	.39149	.39174	.01011	.15438
65	.35377	.33617	.13588	.13718	.22454	.00551
70	.35895	.34140	.21555	.21645	.08281	-.18565
75	.29388	.27591	.22876	.23179	-.06156	.00214
80	.25386	.23668	.11024	.11485	.09251	.12888
85	.22751	.21214	.06647	.07051	.16423	-.02957
90	.13880	.12301	.07787	.08361	.01901	-.04963
95	.12784	.11123	.07264	.08072	.02291	.05043
100	.14811	.13351	.07112	.07794	.08730	.04792
105	.08322	.06858	.03289	.03988	.04685	.01446
110	.06529	.04844	.01424	.02412	.03701	-.00263
115	.10277	.08726	.05487	.06402	.04448	-.01853
120	.07472	.05994	.02133	.02959	-.00962	.00253
125	.09231	.07402	-.06082	-.04934	.02445	-.00453
130	.13024	.11190	-.04532	-.03311	.08730	-.03903
135	.07063	.05282	-.00802	.00445	.03340	-.02182
140	.10507	.08239	-.05551	-.03889	.05184	-.02895
145	.24446	.22178	-.09957	-.08421	.18384	-.04855
150	.20093	.17358	-.11020	-.08947	.11035	.02036
155	.22452	.16848	-.12136	-.06998	-.06338	-.10214
160	.55480	.48221	-.02406	.03964	.04480	-.46369
165	.60370	.56330	.14919	.16809	.22525	-.41428
170	.30522	.26974	.09670	.10641	.15526	.04427
175	.38366	.26715	-.22753	-.12229	.02372	.13513
180	.61027	.42831	-.42831	-.24635	.00000	.00000

$$F_{44}(\Theta) = \sum_{s=0}^{s_{max}} a_4^s P_{00}^s(\cos\Theta), \tag{7}$$

$$F_{12}(\Theta) = \sum_{s=2}^{s_{max}} b_1^s P_{02}^s(\cos\Theta), \tag{8}$$

$$F_{34}(\Theta) = \sum_{s=2}^{s_{max}} b_2^s P_{02}^s(\cos\Theta). \tag{9}$$

In Eqs. (4)–(9), $P_{mn}^s(x)$ are generalized spherical functions.[23,24] Finally, Tables 4 and 5 show the elements of the normalized scattering matrix. The elements of the scattering matrix are also depicted in Fig. 7. Based on the internal convergence checks, we expect that the accuracy of the numbers in Tables 1–5 is within ± 1 in the last digits given.

4. CONCLUSIONS

We have presented and discussed the results of comparisons of laboratory measurements of the scattering matrix elements for a randomly oriented latex bisphere with touching, nearly identical

Table 5. Elements of the normalized scattering matrix vs scattering angle (in degrees) for Model 2.

Θ	F_{11}	F_{22}	F_{33}	F_{44}	F_{12}	F_{34}
0	49.78455	49.77951	49.77951	49.77447	.00000	.00000
5	35.98162	35.97667	35.97626	35.97160	.10705	.13306
10	16.24586	16.24110	16.23787	16.23416	.21533	.23828
15	10.67507	10.67056	10.65748	10.65496	.39163	.34560
20	8.90278	8.89855	8.85575	8.85437	.71344	.48493
25	4.67417	4.67021	4.59943	4.59892	.73578	.30617
30	1.90103	1.89726	1.82180	1.82187	.51177	.01957
35	1.11641	1.11257	1.03461	1.03518	.33577	-.19571
40	1.10229	1.09805	1.03145	1.03264	.15158	-.32446
45	1.13873	1.13393	1.09973	1.10167	.00530	-.26081
50	1.00942	1.00424	.99510	.99766	-.02457	-.11589
55	.85571	.85046	.84877	.85169	.02002	-.00392
60	.64929	.64408	.63356	.63674	.09647	.04628
65	.43570	.43039	.40340	.40693	.14346	.01536
70	.31993	.31440	.27708	.28099	.13643	-.04728
75	.28821	.28250	.24356	.24780	.10457	-.09298
80	.27305	.26716	.23409	.23865	.06754	-.10614
85	.22690	.22087	.19891	.20376	.03623	-.08551
90	.16608	.15991	.14797	.15309	.01953	-.05383
95	.13383	.12732	.12010	.12564	.01720	-.03445
100	.14155	.13466	.12760	.13359	.02517	-.02894
105	.16635	.15925	.14929	.15557	.04271	-.02521
110	.17408	.16672	.14829	.15490	.06852	-.01610
115	.14870	.14109	.10365	.11058	.09019	-.00940
120	.10957	.10169	.03337	.04060	.08931	-.02033
125	.09606	.08760	-.01761	-.00976	.05673	-.05878
130	.13177	.12253	-.01147	-.00280	-.00159	-.11762
135	.20600	.19550	.05854	.06853	-.06144	-.17075
140	.28155	.26925	.16422	.17607	-.08667	-.18663
145	.31664	.30306	.25096	.26414	-.05212	-.14696
150	.29863	.28522	.26592	.27896	.03527	-.06289
155	.25450	.24319	.18699	.19797	.13353	.03002
160	.23308	.22382	.03195	.04092	.19088	.09261
165	.27032	.26186	-.15254	-.14430	.17895	.10303
170	.35827	.34853	-.32017	-.31056	.10971	.07009
175	.45586	.43878	-.43657	-.41953	.03254	.02295
180	.50091	.47807	-.47807	-.45522	.00000	.00000

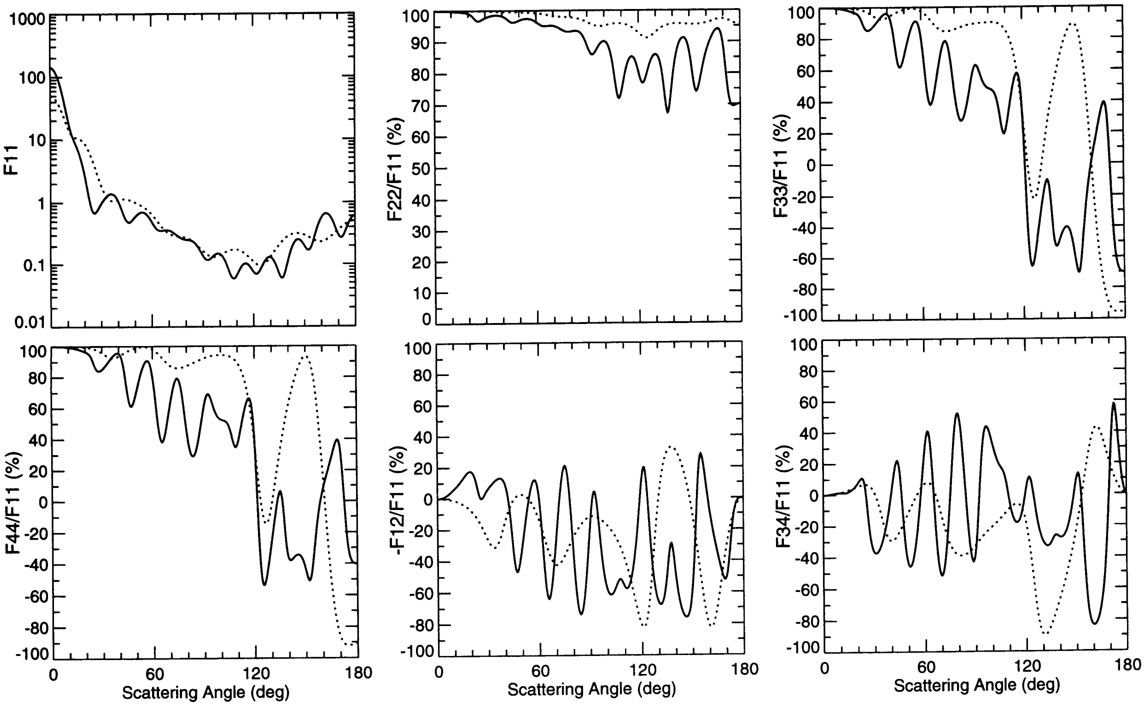

Fig. 7. Elements of the normalized scattering matrix for Model 1 (——) and Model 2 (······).

micron-sized components[5] and numerical computation using the T-matrix method.[6] The overall quantitative agreement between theory and experiment is very good, thus further demonstrating the validity of the numerical technique. Our comparisons also suggest that polarimetric measurements of light scattering can be used as an accurate particle sizing tool (cf. Refs. 25 and 26 and references therein).

We have discussed the reasons that allow us to believe that our T-matrix computer code for bispheres is capable of producing very accurate results. We have used our code to tabulate the efficiency factors and the elements of the scattering matrix for two models of monodisperse, randomly oriented bispheres with touching and separated components and expect that the numbers reported have the accuracy within ± 1 in the last digits given. Because of this high accuracy, our results are suitable for use as benchmarks.

Acknowledgements—The authors thank J. W. Hovenier for valuable comments on an earlier version of this paper. This work was supported in part by the Earth Observing System Project managed by Goddard Space Flight Center in providing for the Earth Observing Scanning Polarimeter instrument and algorithm development and by the NASA Office of Mission to Planet Earth.

REFERENCES

1. G. W. Kattawar and C. E. Dean, *Opt. Lett.* **8,** 48 (1983).
2. K. A. Fuller, G. W. Kattawar, and R. T. Wang, *Appl. Opt.* **25,** 2521 (1986).
3. G. W. Kattawar, C.-R. Hu, M. E. Parkin, and P. Herb, *Appl. Opt.* **26,** 4174 (1987).
4. J. I. Hage, J. M. Greenberg, and R. T. Wang, *Appl. Opt.* **30,** 1141 (1991).
5. J. R. Bottiger, E. S. Fry, and R. C. Thompson, in D. W. Schuerman, Ed., *Light Scattering by Irregularly Shaped Particles*, pp. 283–290, Plenum Press, New York, NY (1980).
6. M. I. Mishchenko and D. W. Mackowski, *Opt. Lett.* **19,** 1604 (1994).
7. M. I. Mishchenko, *JOSA A* **8,** 871 (1991); erratum: *ibid.* **9,** 497 (1992).
8. M. I. Mishchenko, *JQSRT* **46,** 171 (1991).
9. F. Kuik, J. F. de Haan, and J. W. Hovenier, *JQSRT* **47,** 477 (1992).
10. H. C. van de Hulst, *Light Scattering by Small Particles*, Wiley, New York, NY (1957).
11. A. Ishimaru and Y. Kuga, *JOSA* **72,** 1317 (1982).
12. J. W. Hovenier, H. C. van de Hulst, and C. V. M. van der Mee, *Astron. Astrophys.* **157,** 301 (1986).
13. C. R. Hu, G. W. Kattawar, M. E. Parkin, and P. Herb, *Appl. Opt.* **26,** 4159 (1987).
14. M. I. Mishchenko and L. D. Travis, *Appl. Opt.* **33,** 7206 (1994).

15. E. S. Fry and G. W. Kattawar, *Appl. Opt.* **20,** 2811 (1981).
16. C. V. M. van der Mee and J. W. Hovenier, *Astron. Astrophys.* **228,** 559 (1990).
17. M. I. Mishchenko, D. W. Mackowski, and L. D. Travis, *Appl. Opt.* **34,** 4589 (1995).
18. P. J. Flatau, K. A. Fuller, and D. W. Mackowski, *Appl. Opt.* **32,** 3302 (1993).
19. P. J. Flatau, private communication (1994).
20. K. A. Fuller, *Appl. Opt.* **30,** 4716 (1991).
21. V. P. Tishkovets, *Kinem. Fiz. Nebes. Tel* **10**(2), 58 (1994).
22. J. F. de Haan, P. B. Bosma, and J. W. Hovenier, *Astron. Astrophys.* **183,** 371 (1987).
23. I. M. Gel'fand, R. A. Minlos, and Z. Ya. Shapiro, *Representations of the Rotation and Lorentz Groups and their Applications*, Pergamon Press, Oxford (1963).
24. J. W. Hovenier and C. V. M. van der Mee, *Astron. Astrophys.* **128,** 1 (1983).
25. F. Kuik, P. Stammes, and J. W. Hovenier, *Appl. Opt.* **30,** 4872 (1991).
26. J. L. Huckaby, A. K. Ray, and B. Das, *Appl. Opt.* **33,** 7112 (1994).